

Molecular dynamics study of the effect of sodium and chloride ions on water-surfactant-hydrocarbon interfaces

Anastasia A. Ivanova ^{a,b,*}, Alexey N. Cheremisin ^b, Ahmed Barifcane ^a, Stefan Iglauer ^d, Chi Phan ^c

^a Western Australian School of Mines (WASM): Minerals, Energy and Chemical Engineering, Curtin University, 26 Dick Perry Avenue, Kensington 6151, Australia

^b Center for Hydrocarbon Recovery, Skolkovo Institute of Science and Technology, 3 Nobel Street, 121205 Moscow, Russia

^c Discipline of Chemical Engineering, Curtin University, Kent Street 6102, Bentley, Australia

^d School of Engineering, Edith Cowan University, 270 Joondalup Drive, 6027 Joondalup, Australia

ARTICLE INFO

Keywords:

Interfacial tension
Molecular dynamic simulations
Salinity and temperature effects
Cationic surfactants
CTAC
EHAC

ABSTRACT

Molecular dynamic simulations have been performed to study the effect of electrolyte concentrations and temperature on the structural, dynamic, and thermal properties of cationic surfactants at the water/n-decane interface. Results show that optimal salinity (where the interfacial tension (IFT) passes through a minimum) could be reached for erucylbis-(hydroxyethyl)-methylammonium chloride (EHAC). In contrast, the IFT of cetyltrimethylammonium chloride (CTAC) solution increased for all NaCl concentrations tested. It was demonstrated that above optimum salinity, EHAC molecules were repelled from the interface due to Na^+ diffusing closer to the Stern layer and contributing to the positive interfacial charge, resulting in micelle formation in the bulk phase. However, CTAC molecules moved further inside the hydrocarbon phase upon salt addition. These findings provide an important basis for studying surfactant interfacial behavior as a function of salinity, so that better formulations can be developed for applications where salinity is non-zero, e.g. in pharmacy or enhanced oil recovery.

1. Introduction

The adsorption of amphiphilic surfactant molecules at a liquid/liquid interface is an essential process that is not only of fundamental interest but also of practical importance in a wide range of industrial applications, including chemical and biological systems [1,2] or petroleum production [3,4]. One of the main reasons for using surfactants in technological processes, such as emulsification/demulsification and stabilization/destabilization of oil-in-water and water-in-oil emulsions, is their ability to self-assemble at phase interfaces, which leads to the reduction of the interfacial and surface tensions. Importantly, the self-assembly of surfactants plays a key role in the mobilization of oil trapped in rock pores in the context of chemically enhanced oil recovery [5]. However, the functionality of surfactant formulations, and consequently, oil recovery efficiency, strongly depends on the concentration and type of ions present in the formation brine [6]. In general, the presence of salt in natural brines causes a decrease in the solubility of surfactants in the aqueous phase due to the salting-out effect [7,8]. Thus, more surfactant molecules are forced to approach the interface, which leads to a brine/oil interfacial tension (IFT) decrease. In addition, ions

can enhance the packing of surfactant molecules at the interface due to the counter-ion screening effect between similarly charged surfactant heads, resulting in further brine/oil IFT reduction [9]. Indeed, an increase in NaCl concentration from 10000 ppm to 100000 ppm in aqueous cationic surfactant (nominally 1-dodecyl-3-methylimidazolium chloride) formulations gradually reduced aqueous phase/oil IFT [8]. This reducing trend was attributed to the neutralization of surface charges on the surfactant heads with oppositely charged counter-ions [8]. As a result, the accumulation of surfactant molecules at the interface increased, leading to IFT reduction. A decrease in surfactant/paraffin IFT was also reported for increasing MgCl_2 , NaCl , NH_4Cl , and LiCl contents measured up to 0.2 M concentration in the aqueous phase [10]. The same decreasing trend was also identified for aqueous anionic surfactant (fatty alcohol polyoxyethylene ether carboxylate) solutions when NaCl concentration was increased from 0.1 M to 0.5 M [11]. Moreover, the IFT between petroleum sulfonate and heavy oil (and also the 'oil's polar components, i.e. resins and asphaltenes) was found to decrease rapidly (from 8.5 to 1 mN/m) when NaCl concentration was below 0.2 M and more slowly (from 1 to 0.01 mN/m) at higher NaCl contents [12]. It was suggested that the presence of salt promoted and

* Corresponding author at: Center for Hydrocarbon Recovery, Skolkovo Institute of Science and Technology, 3 Nobel Street, 121205 Moscow, Russia.
E-mail address: anastasia.ivanova@postgrad.curtin.edu.au (A.A. Ivanova).

accelerated the diffusion of petroleum sulfonate molecules to the oil/water interface, resulting in interfacial activity increase, with a consequent IFT decrease [12].

In contrast, Liu et al. [11] found a minimum of IFT between *n*-decane and aqueous fatty alcohol polyoxyethylene carboxylate surfactant solutions when NaCl concentration was increased, clearly exhibiting a V-shaped curve. This observation is supported by the results of Kumar and Mandal [9] who reported that surfactant/oil IFT passes through a minimum with increasing NaCl content in anionic (sodium dodecyl sulfate - SDS) and cationic (cetyltrimethylammonium bromide - CTAB) surfactant solutions. Notably, such a V-shape of IFT as a function of NaCl concentration was also observed for non-ionic surfactants [13]. Bera et al. associated the decrease in IFT with in situ formation of surface-active agents when NaCl salt was added [13].

However, despite a considerable number of experimental studies, the existence of two different IFT-salinity patterns cannot be satisfactorily explained. For instance, while the descending IFT trend can be attributed to the surfactant molecules packing tightly at the interface, the ascending IFT trend is not well understood. Bera et al. [13] suggested that IFT starts to increase when the accumulation of surface active-agents at the interface reaches a saturation point. Another promising explanation is the partitioning of surfactant molecules into the oil phase as salinity increases, with a consequent formation of micelles in the oil phase [14].

Due to complexities associated with the experimental procedures and limitations of experimental equipment, it is challenging to investigate the effect of ions at the atomic scale in such systems and capture their precise molecular arrangements at the interface, especially in the presence of surfactants [15]. Recently, it was shown that molecular simulations such as molecular dynamics (MD) and Monte Carlo (MC) could be used to describe the molecular interactions and orientations at liquid/vapor [15–18] and liquid/liquid [19–22] interfaces at the atomic scale. Thus, these methods have been effective tools for providing detailed atomistic and molecular information at such interfaces, including hydrogen bond correlation functions [23] and interfacial thicknesses [24]. Although these simulations addressed the influence of ions on brine/oil [25] and surfactant/brine/oil IFT [26], to our knowledge, no systematic MD study has been performed to investigate the effect of ions and temperature on the interfacial properties of surfactants with different molecular architecture at the hydrocarbon/water interface.

Therefore, to address this knowledge gap, we present MD simulation studies on ions and temperature effects for better understanding of adsorption processes at the water/hydrocarbon interface. The surfactants used in this study were both cationic (erucylbis-(hydroxyethyl)-methylammonium chloride, EHAC, and cetyltrimethylammonium chloride, CTAC). EHAC has two hydroxyl groups (Fig. 1), and thus, can have the characteristics of both cationic and non-ionic surfactant. EHAC is also known to enhance the viscosity (up to 10^4 Pa*s) and viscoelastic properties of aqueous solutions in the presence of salt, and therefore, has been extensively tested for hydraulic fracturing applications [27,28]. Notably, our previous experimental studies showed that EHAC is also a promising surfactant for enhanced oil recovery (EOR) applications for either lowering water/oil IFT or increasing the viscosity of injected fluids [28,29]. However, temperature and ion influence on EHAC performance remains unclear due to the complex molecular structure of the EHAC head group. CTAC, which is also a cationic surfactant, is selected for comparison. This study thus focuses on the following aspects: how surfactant packing at the water/oil interface is affected by ion-specific effects and how temperature influences the molecular arrangements and interactions of surfactant molecules at the interfacial zone in the presence of sodium and chloride ions.

2. Computational method

The interfacial behavior of the cationic surfactants CTAC and EHAC

has been studied by molecular dynamics. Simulation boxes were built by placing slabs of surfactant layers (2 nm each) around an *n*-decane layer (thickness 6 nm). The model system consisted of two *n*-decane–aqueous phase interfaces, as this has been shown to be advantageous for liquid/liquid interfacial studies [30,31]. The box with surfactant and *n*-decane molecules was stretched along the Z direction to 18 nm to create space for water molecules. Owing to the fact that formation water is usually enriched mainly with NaCl salt [32], different numbers of Na⁺ and Cl⁻ ions were inserted by replacing water molecules so that prescribed salt concentrations were reached (i.e. NaCl concentrations of 0.01, 0.02, 0.03, 0.05, 0.07, 0.1, 0.2, 0.4, 0.6 and 1 M). This range of NaCl concentrations accounts for low salinity brine (5 wt%) and a typical reservoir brine salinity [25]. The number of surfactant molecules in each slab was set so that area density for EHAC equaled to 0.25 molecule / nm² and for CTAC 0.38 molecule / nm². These values were adopted from previous simulation studies and are consistent with other simulations of the surfactant layers [20,33,34,35]. An increase in surfactant concentration will lead to the formation of aggregates (micelles) in bulk, which is dominated by tail-tail interactions [23,40,41].

Furthermore, at higher surfactant concentration, some molecules will move to the bulk [43], and thus, RDF functions and density profiles of atoms at interfacial zone cannot be analyzed separately from those in bulk. These values were kept constant in all simulation runs. Since our study focused on molecular interactions at the interface (and not on the bulk properties of surfactants), the concentrations considered in this study are within a reasonable range to mimic the adsorption behavior and chemical interactions properly.

The partial charge distribution among atoms and ions (Fig. 1) was taken from data proposed in the literature [36], where similar systems were computationally analyzed [34]. The molecular potentials between atoms of both surfactants were described by the GROMOS force field [37,42]. The SPC/E model was employed to model the water potential [38], and the particle-mesh Ewald (PME) method of summation was implemented to compute the electrostatic interactions [39]. The initial

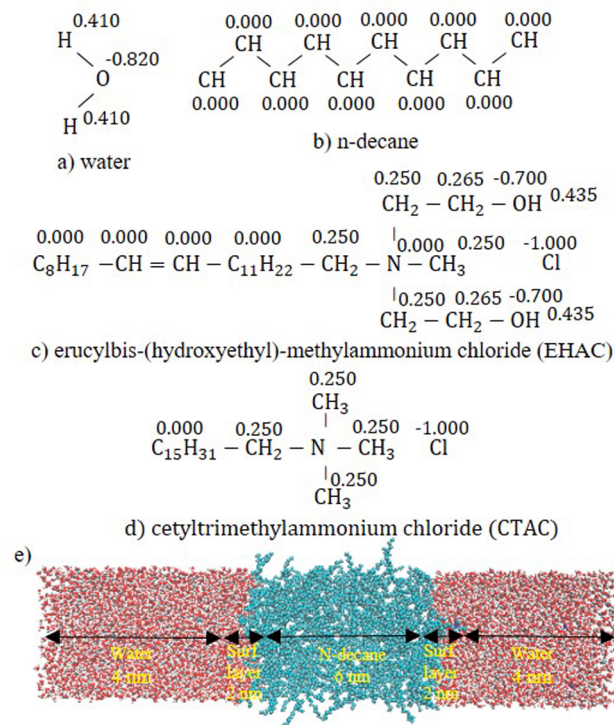


Fig. 1. Chemical structures and charge distribution models used in this study: a) water; b) *n*-decane; c) erucylbis-(hydroxyethyl)-methylammonium chloride and d) cetyltrimethylammonium chloride; e) simulation box.

size of the simulation box was $4 \times 4 \times 18 \text{ nm}^3$ for each system.

All molecular dynamic simulations were carried out using the GROMACS 4.5.5 package [42] at atmospheric pressure (1 bar) and two temperatures (298 K and 343 K). The steepest descent method with the cut-off scheme for Coulomb and van der Waals forces of 0.9 nm was used for energy minimization to ensure that the system had no steric clashes. The first step of equilibration was conducted under an NVT ensemble (constant number of particles, volume, and temperature) using a Berendsen thermostat [39]. Equilibration of the pressure, and thus also density, were performed under an NPT ensemble (constant number of particles, pressure, and temperature) using the Parrinello-Rahman barostat [39]. The calculated densities of *n*-decane (0.726 g/ml) and water (0.994 g/ml) are in a good agreement with experimental values – 0.725 g/ml and 0.997 g/ml [54,60,61]. Both NVT (200 ps) and NPT (500 ps) equilibration steps were carried out at 1 bar, and the temperature studied (i.e. 298 K and 343 K), followed by 20 ns of production runs in the NVT ensemble using the Nose-Hoover thermostat [39]. The interfacial tensions, density profiles, distribution functions of *n*-decane, ions and surfactants, and the number of hydrogen bond was calculated by analyzing the atomic trajectories recorded at 0.5 ps intervals. The last 2 ns of total simulation time (20 ns) has been collected for accurate IFT calculation processing.

3. Results and discussion

3.1. Effect of ions and surfactant molecular structure on water/hydrocarbon interfacial behavior

The interfacial tension (γ) can be determined from Eq.1 [30], as the interface between the phases is perpendicular to the Z-axis direction:

$$\gamma = - \int_0^{L_z} (p'(z) - p) dz \quad (1)$$

where L_z is the box length along the z-axis, $p'(z)$ is the lateral pressure, and p is the bulk pressure.

The integral in Eq.1 can be calculated using the fact that in the bulk solution $p = p'(z)$ and taking into consideration that there are two interfaces in our system:

$$\gamma = -\frac{1}{2} \left(\frac{p_x + p_y}{2} - p_z \right) L_z \quad (2)$$

where p_α describes the three diagonal elements of the pressure tensors $P_{\alpha\alpha}$ ($\alpha = x, y, z$) along the axis.

Hence, the simulation data for the water/*n*-decane interfacial tensions in the presence of EHAC and CTAC surfactants at different NaCl concentrations are presented in Fig. 2a,b. In order to obtain accurate values, only the last 2 ns of simulation data was used for IFT calculation (Fig. 2a,b). The standard deviation was calculated based on data collected from at least three independent simulation runs for each salt concentration.

The water/NaCl/EHAC/*n*-decane system's interfacial tension went through a minimum at 0.03 M NaCl concentration, illustrating a V-shaped pattern at 298 K and 343 K (Fig. 2c). On the other hand, the water/NaCl/CTAC/*n*-decane system's interfacial tension increased within the range of all tested NaCl concentrations at 298 K and 343 K (Fig. 2d).

Notably, the same V-shaped pattern has been experimentally observed by the authors studying the salt effect on IFT of CTAB, SDS, and Tween 80 surfactants [9]. The optimal salinity salt concentrations (when IFT passed through the minimum) have been found for all surfactants. Interestingly that the value of optimal salt concentration is different for surfactants, and the authors proposed several explanations. As such, the decrease in IFT by the addition of NaCl to Tween 80 mixture is explained by weakening the hydrogen bonds. Whereas in the case of ionic surfactants CTAB and SDS the main reason for IFT reduction is due to a decrease in the electrical repulsion between charged head groups, resulting in decreasing the size of the micelle in the present of ions [9].

Here, we exclude the influence of impurities or synergy effects of different hydrocarbons on interfacial behavior as all simulations were performed with the pure components. Therefore, one of the main

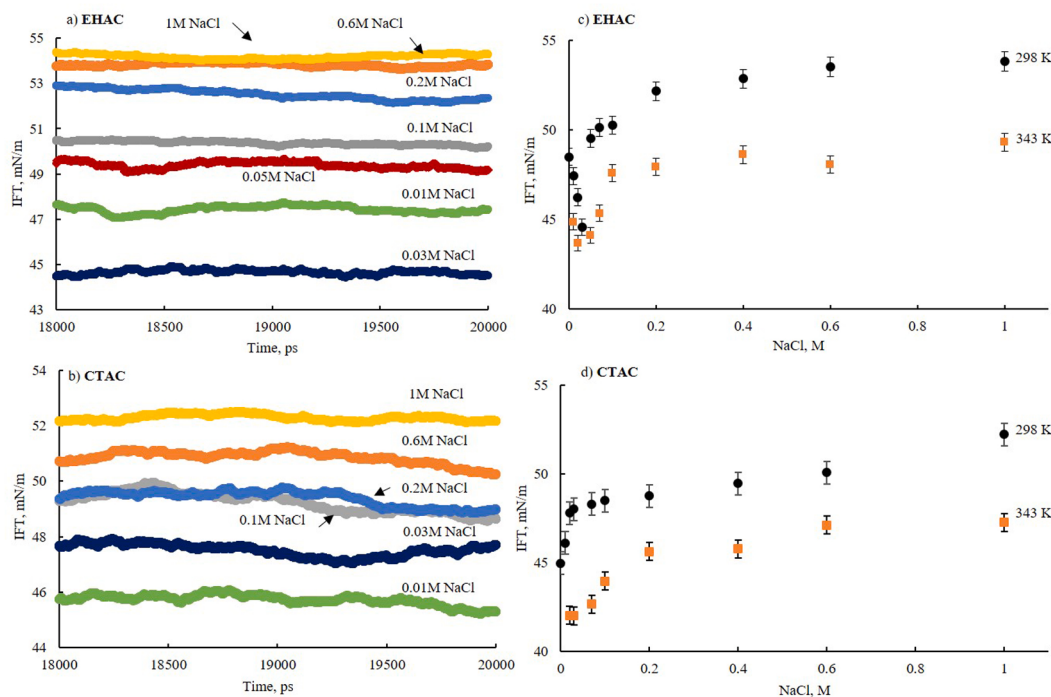


Fig. 2. Simulation data for the water/*n*-decane interfacial tension in the presence of (a,c) EHAC surfactant and (b,d) CTAC surfactant at different NaCl concentrations; calculated IFT values for EHAC (c) and CTAC (d) surfactants as a function of NaCl concentration at two different temperatures – 298 K (black circles) and 343 K (orange squares). Note (a) and (b) represent data simulated at 298 K.

reasons for the observed ascending IFT trend for CTAC could be related to an emulsion inversion from oil-in-water (o/w) to water-in-oil (w/o), which is caused by an increase in salt concentration. Indeed, this behavior is usually described in terms of the Winsor phase types [43,44]. As such, if surfactant forms an o/w emulsion in the aqueous phase, it is affiliated with a Winsor I system; in contrast, a system with w/o emulsion formed in the oleic phase is referred to as Winsor II type. However, Winsor I or Winsor II emulsions exhibit high IFT values [44], as surfactant molecules are mostly retained in bulk (water or oil) phases rather than at the interface. Instead, low IFT values can be reached when there is a continuous layer of surfactant molecules between aqueous and oleic phases, referred to as Winsor Type III behavior. Previously it was reported that without salt, all CTAC molecules tend to adsorb at the interface, representing Winsor Type III behavior [20]. In this context, we suggest that water/CTAC/*n*-decane systems in the presence of electrolytes endured the behavioral inversion from a Winsor III (when all CTAC molecules were adsorbed at the interface) to a Winsor II system. Such a salting-out effect can be governed by temperature [20,45] and/or salinity [46]. Therefore, the solubility of CTAC in the water phase is lowered due to an increase in salt content, and, as a result, CTAC affinity to the oil phase is relatively increased. This is also verified by observing slight diffusion of CTAC molecules further inside the oil phase (see below sections). Consequently, IFT increased upon salt addition.

It is worth mentioning that in our study, we used NaCl concentrations between 0.01 and 1 M. Although this is consistent with the NaCl content in the reservoir brines [25], even the lowest tested NaCl concentration may be too high to observe the descending IFT trend of CTAC. For instance, Zhang et al. [47] experimentally showed that emulsion inversion in systems containing sorbitan oleate surfactant occurred at significantly lower NaCl concentrations, around 5 mM.

Interestingly, the IFT of water/NaCl/EHAC/*n*-decane systems exhibited different behavior (Fig. 2a). In some experimental studies on IFT of the electrolytes/surfactant solution/oil, the IFT has been found to pass through a minimum with increasing salinity [9,11,13]. However, in these previous studies, only two regions were observed - IFT decreased in the first region upon addition of salt up to the optimal salt concentration, then IFT increased again with further salt concentration increase in the second region. The resulting IFT-salinity curve illustrated a V-shaped pattern.

Here, the existence of a third region on the IFT-salinity curve has been evidenced. In this region, IFT values remained almost unchanged at higher salt concentrations (Fig. 2c). Indeed, when NaCl concentration was higher than 0.4 M, IFT remained almost constant and varied in the range 52.16 – 54.27 mN/m (Fig. 2c). This range is consistent with experimental data of the interfacial tensions between brine solutions and hydrocarbons [48]. Therefore, we suggest that this phenomenon is attributed to the repulsion of almost all surfactant molecules from the interface into the bulk due to the presence of Na^+ ions near the interface. To substantiate this further, we calculated the density distribution profiles and studied micelle formation in the bulk (see below sections).

Notably, for EOR applications, reservoirs with temperatures ranging from 343 K to 393 K are

considered to be promising candidates for surfactant flooding [53]. Therefore, in our study, we investigated the effect of one of the typical reservoir temperatures (343 K) on the interfacial properties of the surfactant systems. Clearly, the IFT patterns for both surfactants at 343 K followed the same trend as obtained for 298 K (Fig. 2c,d).

3.2. Arrangement of water molecules at the interface

It is interesting to point out that the surface tension between water and air in the presence of electrolytes also passes through a minimum at very low salt concentrations (1–2 mM) [49]. This effect is known as the Jones-Ray effect and has been considered an experimental artifact until recent experiments, including non-resonant second harmonic scattering and surface ion resonant second-harmonic reflection measurements,

confirmed its existence [49]. The authors [49] attributed this effect to the increase of the orientational order of water molecules in bulk induced by ions' addition, which in turn increased the entropic penalty that caused the reduction of the surface tension.

Thus, following Okur et al. [49], we suggest that the descending trend of EHAC IFT at low salt concentrations (<30 mM) originates from the increasing orientational order of water molecules due to ion-dipole electrostatic interactions either in bulk or near to the interface. To explore this further, in this study, the orientation of water molecules at the *n*-decane/water interface in the presence of EHAC and different NaCl concentrations was analyzed considering the water dipole order parameter, $\cos(\theta)$, where θ is the angle between Z-axis and water dipole moment [50]. The simulation box was divided into slices, with each water molecule assigned to a slice per time frame, and the average orientation per slice was calculated. Fig. 3 illustrates the computed average $\cos(\theta)$ as a function of distance along the Z-axis. The results demonstrated that $\cos(\theta)$ values remained positive at the interfacial zone, forming a peak. At the same time, the bulk angle equaled zero due to the random distribution of water molecules (Fig. 3). Note that the same trends of $\cos(\theta)$ were observed for ethanol and methanol at the water/air interface [50,51].

It was shown [52] that near the interface, water molecules have a two-layer orientation, namely in one layer, the water molecules pointed towards the water phase, while they pointed towards the oil phase in another layer. The presence of surfactant molecules and ions near the interface disrupted this molecular water molecule arrangement. Therefore, water molecules at the outmost layer tended to reorient to comfort EHAC molecules and ions [50]. It can be seen in Fig. 3 that the positive peak increased and shifted further inside the *n*-decane phase with increasing NaCl concentrations up to 0.03 M, which suggests an increase in the orientational order of water molecules. This shift of the peak in the water dipole order distribution curve has been correlated with the surface tension reduction [50–52]. Thus, the decrease of IFT upon the addition of NaCl below 0.03 M can be attributed to the increase of the water's orientational order.

3.3. Density distribution profiles of surfactants, *n*-decane, ions and water

Average density distribution profiles were obtained for water, *n*-decane, either EHAC or CTAC surfactant, and Na^+ and Cl^- ions by calculating their density values over 300 slices perpendicular to the Z-axis. The bulk density of water was found to increase slightly with the increase of NaCl concentration, while the bulk density of *n*-decane was calculated to be 726 kg/m³. Both are in good agreement with literature data [54].

It can be seen in Fig. 4 that EHAC and CTAC surfactant molecules

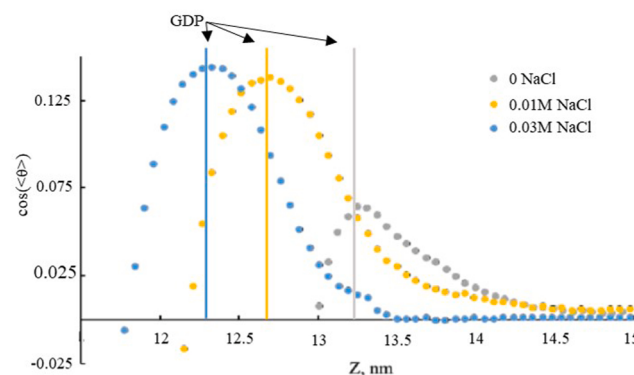


Fig. 3. Water dipole order parameter in the presence of EHAC molecules for different NaCl concentrations. Gibbs dividing planes are shown for each salt concentration accordingly. Colors represent 0 NaCl (grey), 0.01 M NaCl (yellow) and 0.03 M NaCl (blue).

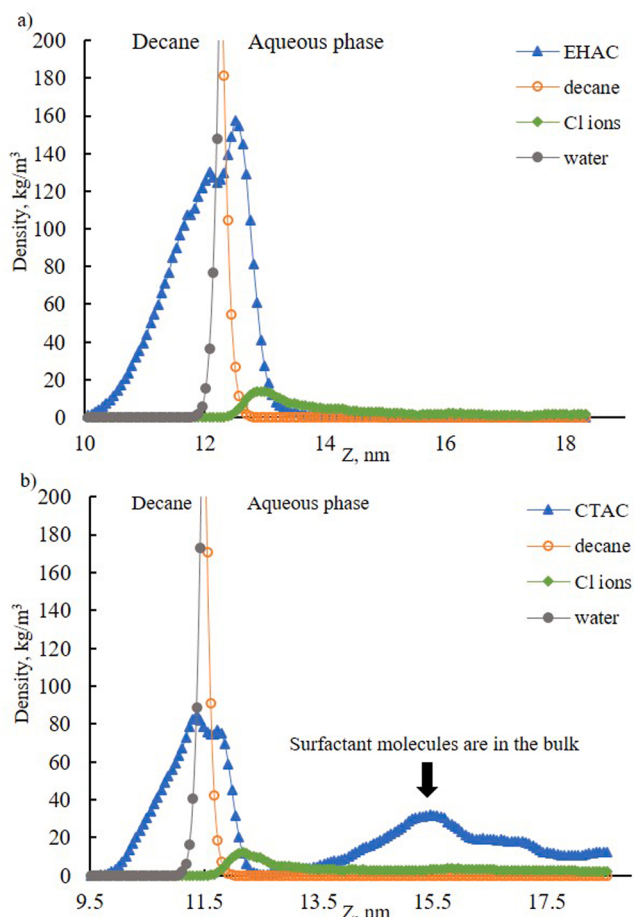


Fig. 4. Density profiles of water/n-decane systems containing (a) EHAC surfactant and (b) CTAC surfactant in the presence of 0.01 M NaCl.

were oriented around the water/n-decane interface with two well-defined sharp peaks. The right peak represented the surfactants' head polar groups anchored in the water phase, while the left peak corresponded to the hydrophobic tail, which resided inside the n-decane phase.

Interestingly, at low salt concentrations (<0.03 M), no EHAC molecules were observed in the bulk phase, whereas CTAC molecules were located both at the interface and in bulk, illustrating a different behavior (Fig. 4b). Note that in the absence of salt, CTAC surfactant molecules are adsorbed only at the water/n-decane interface at 298 K [20].

Therefore, to describe the surfactant molecules' interfacial behavior, we analyzed the distributions of surfactant tails and heads at the interface at different salt concentrations (Fig. 5). The Gibbs dividing planes were determined for each salt concentration by fitting the simulated water density data of the interfacial zone with the error function [55] (Eq. (3)):

$$\rho(z) = \frac{\rho_0}{2} \left(1 - \text{erf} \left(\frac{z - z_0}{\sqrt{2w}} \right) \right), \quad (3)$$

where ρ_0 is the water density, z_0 is the position of the Gibbs Dividing Plane (GDP), erf is an error function and w is the interfacial width.

The density profiles of surfactants and Cl⁻ ions in 0.01 M and 0.1 M NaCl brines are shown in Fig. 5a,b. The distances of surfactant tails and heads relative to the GDP position are plotted as the NaCl concentration function in Fig. 5c,d. Note, highest peaks of density profiles have been used for distance calculation.

As can be seen in Fig. 5, EHAC and CTAC molecules were arranged differently at the interfacial zone when salt concentration was increased. As such, the polar heads of EHAC approached closer to the interface from 0.24 nm to 0.16 nm when NaCl concentration was below 0.03 M, and moved further inside the aqueous phase when NaCl was above 0.03 M (Fig. 5c). This trend clearly followed the IFT V-pattern (Fig. 2c), and thus the decrease in IFT at low salt concentrations can be attributed to the optimal packing of surfactant heads at the interface that allows more surfactant molecules to adsorb. However, with further NaCl concentration increase, the distance between head and interface started to increase, whereas the distance between tail and interface gradually decreased. Therefore, we conclude that some surfactant molecules desorbed from the interface, and fewer surfactant molecules were present at

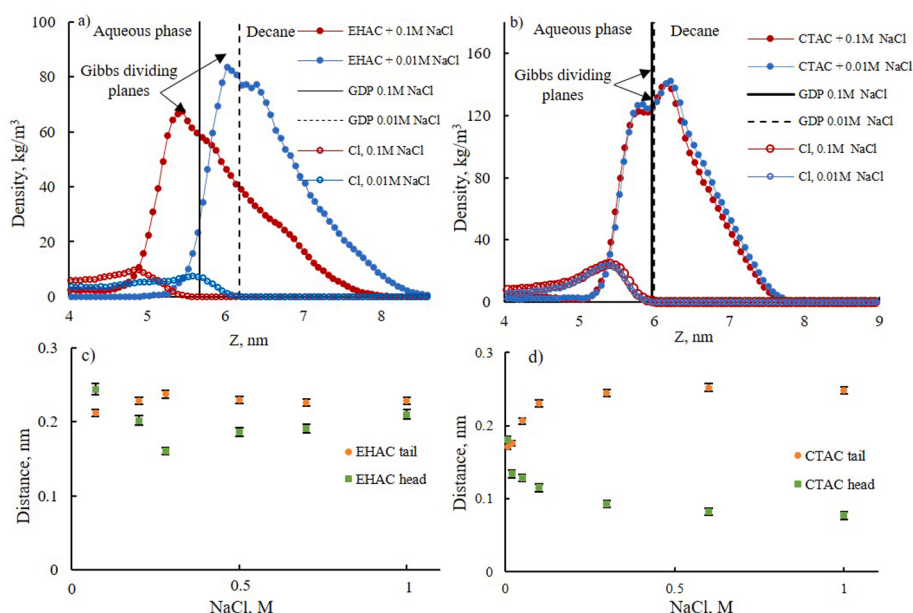


Fig. 5. Surfactant and ion density distributions: (a) EHAC surfactant and (b) CTAC surfactant in the presence of 0.1 M NaCl (red circles) and 0.01 M NaCl (blue circles); distance of surfactant tail and head relative to the GDP position as a function of NaCl concentration: (c) EHAC surfactant and (d) CTAC surfactant.

the interface, resulting in the IFT increase. When almost no surfactant molecules were left at the interface, IFT values were identical to experimental values for the NaCl brine/hydrocarbons system within the experimental error [56].

In contrast, an increase in NaCl concentration in water/*n*-decane systems containing CTAC showed the opposite behavior. While the distance between the surfactant head and interface decreased, the distance between the tail and interface increased (Fig. 5d). We conclude that CTAC molecules penetrated further inside the oil phase with increasing NaCl content. As a result, IFT increased for all NaCl concentrations investigated (Fig. 2d). The same behavior was experimentally observed for the IFT between anionic decylmethylnaphthalene sulfonate surfactant and crude oil [14]. It was suggested [14] that at high salinity (>0.4 M), surfactant molecules start to partition into the oil phase, resulting in the formation of reverse micelles.

Taking into account that CTAC surfactant cannot form hydrogen bonds with water molecules (see below section for an explanation), we propose that the main reason for the IFT increase in the presence of salt is that the hydrophobic interactions become stronger than the solute–solvent interactions, and thus, surfactant molecules migrate into the oil phase.

The different interfacial arrangements of EHAC and CTAC are also visualized in Fig. 6. It can be seen in Fig. 6 that at 1 M NaCl concentration, all EHAC molecules associated with each other and formed micelles, while no CTAC micelle was observed either in the oil or in the aqueous phase (Fig. 6c,f). This can be explained by the different molecular surfactant structure, which results in different critical micelle concentrations (CMC), which are 0.03 mM for EHAC [27] and 0.92 mM for CTAC [57]. Besides, CMC is found to decrease with the addition of salt [43], which also facilitates EHAC micelle formation in the bulk phases. However, in Fig. 6f, it can be seen that although CTAC micelles were not found in the oleic phase, surfactant molecules moved further inside the hydrocarbon phase.

A fundamental question of interest here is the Na^+ ion distribution, which we hypothesize to be the main reason for the surfactant molecules being repelled from the interface. To verify this hypothesis, we analyzed the Na^+ density distribution profiles at different NaCl concentrations relative to the Gibbs dividing plane (Fig. 7).

Interestingly (Fig. 7c,d), at high NaCl concentration (1 M), Na^+ ions

approached the interface more closely in the presence of EHAC (1.55 nm distance) than in the presence of CTAC (2.06 nm distance) molecules. On the contrary (Fig. 7a,b), at low NaCl concentration (0.1 M) Na^+ ions were distributed homogeneously in bulk in the case of both surfactants.

It is known that positively charged surfactant headgroups adsorbed at the interface facilitate the adsorption of negatively charged Cl^- ions in the Stern layer of the same Helmholtz plane [59]. Furthermore, adsorbed ions can be shared by several headgroups, and thus the Stern layer is not electroneutral. The charge of the Stern layer (i.e. the sum of charges of adsorbed surfactant headgroups and ions) determines the potential of the diffuse layer. Thus, as outlined above, with increasing salt concentration, Na^+ ions can approach closer to the interface (out of the diffuse layer), contributing to the overall positive interfacial charge density. As a result, cationic surfactant molecules are repelled from the interface due to the increased positive charge density. These results are conceptionally illustrated in Fig. 8.

Clearly, the interfacial behavior of CTAC differs from that of EHAC. One can suggest two reasons for this. First, the surfactants have different chemical head and tail structures, which impact interfacial arrangement and orientation. Second, the studied CTAC concentration and salt range (0.01 – 1 M) may be insufficient for observing CTAC micelle formation. However, according to the density distribution profiles (Fig. 5), we suggest that CTAC molecules diffused slightly into the oil phase due to the salting-out effect, resulting in a decrease in the surfactant's affinity towards the aqueous phase.

3.4. The interfacial thickness of aqueous, hydrocarbon, and surfactant phases

On the basis of the density distribution profiles (Fig. 4), we calculated and analyzed the interfacial thicknesses of the different phases of the system. Fig. 9a presents the density distribution profiles of *n*-decane, water, EHAC surfactant and Cl^- ions (NaCl concentration corresponded to 0.01 M) along the Z-axis. It is a common practice to characterize the total thickness (h_{total}) of the system by using the “90–90” criterion [24], where h_{total} is calculated as the distance between two points where the densities of oil and water are 90% of their bulk densities (which are 725 kg/m^3 [60] and 997 kg/m^3 [61] for *n*-decane and water, respectively). Generally, for calculation of the interfacial thicknesses of the oil (h_{oil})

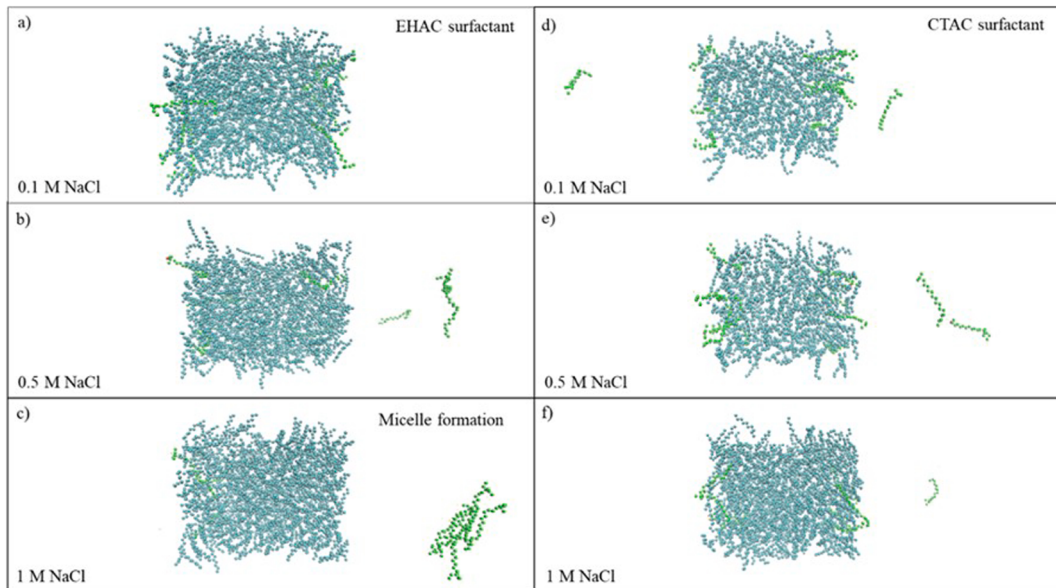


Fig. 6. Snapshots (obtained using VMD [58]) of the simulation box containing EHAC surfactant with (a) 0.1 M NaCl, (b) 0.5 M NaCl and (c) 1 M NaCl brine; CTAC surfactant with (d) 0.1 M NaCl, (e) 0.5 M NaCl and (f) 1 M NaCl brine. Colors: cyan – carbon in *n*-decane, green – carbon in surfactant. Water molecules and ions are removed for the better visualization.

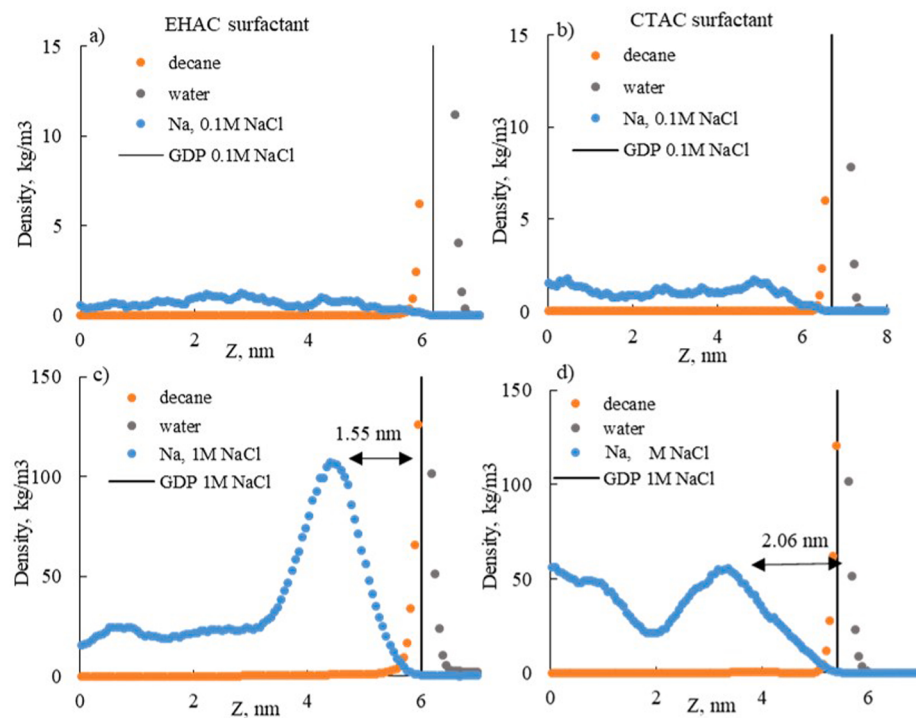


Fig. 7. Average density distributions of decane (orange circles), water (grey circles) and Na⁺ ions (blue circles) for EHAC (a, c) and CTAC (b, d). Note that NaCl concentration is 0.1 M in (a), (b) and 1 M in (c), (d).

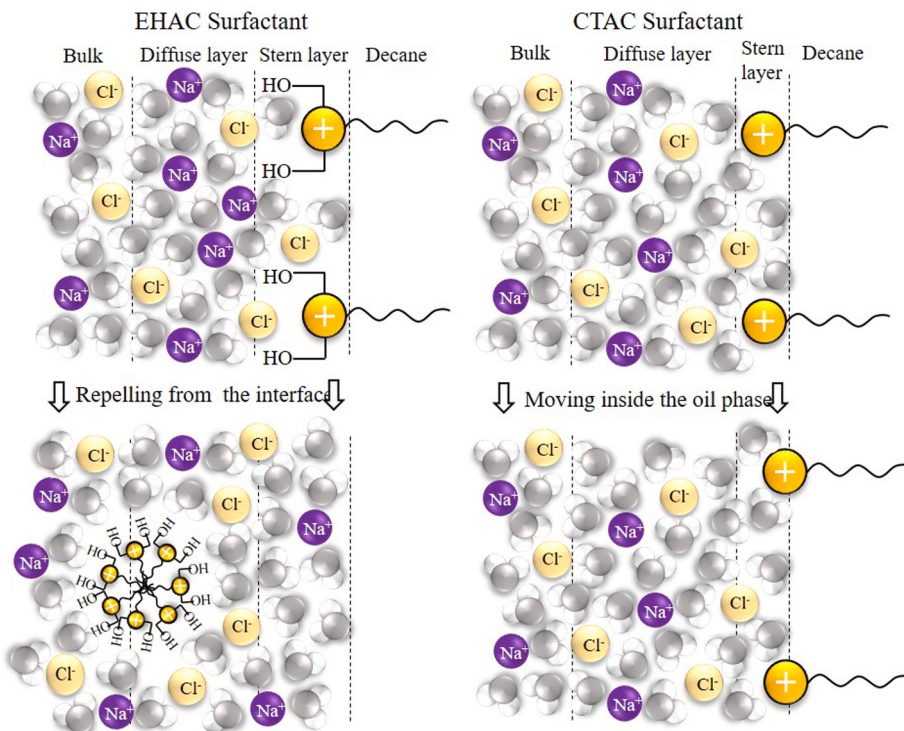


Fig. 8. Schematic representation of ion and surfactant molecule arrangements at the interface, in the diffuse layer, and in the bulk phase at high salt concentrations. Colors represent: water molecules (white and grey), Na⁺ (purple), Cl⁻ (yellow), surfactant head (orange).

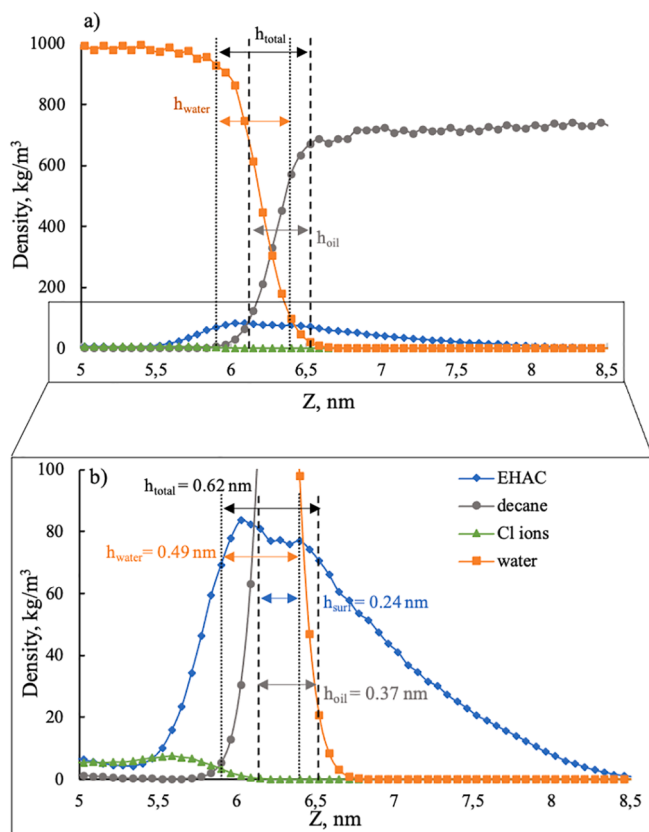


Fig. 9. (a) Density profiles of *n*-decane, water, EHAC surfactant, and Cl ions; (b) Zoom into area highlighted by the black rectangle in (a) (note that the NaCl concentration was 0.01 M).

and water (h_{water}) phases, a "10-90" criterion is used, where the thickness is measured as a distance between two points corresponded to a density difference from 10 to 90% of the bulk phase. This concept is illustrated in Fig. 9a. As such, the h_{total} , h_{oil} and h_{water} were calculated as 0.62 nm, 0.37 nm, and 0.49 nm, respectively (Fig. 9b).

The presence of surfactant at the interface results not only in the formation of two sub-interfaces (oil/surfactant and water/surfactant) but also in a surfactant monolayer (h_{surf}) [24]. Thus, the interface consists of the three layers h_{surf} , h_{oil} and h_{water} , where h_{oil} and h_{water} are determined by "10-90" criteria for *n*-decane and water phases, respectively, and h_{surf} is calculated as $h_{surf} = h_{water} + h_{oil} \cdot h_{total} = 0.24$ nm. The same methodology was used for thickness calculations of CTAC systems.

Using the "10-90" criterion the total interfacial thickness of the *n*-decane/water system without surfactant was found to be 0.49 nm, which is in good agreement with the experimentally measured value (0.46 nm) [62], and independent MD simulations [30]. Thicknesses of oil (h_{oil}) and water (h_{water}) interfaces were 0.41 nm and 0.46 nm, respectively.

It can be seen in Fig. 9 that the addition of EHAC surfactant resulted in broadening of h_{total} by 0.13 nm. Such an increase illustrates the well-known effect of surfactant adsorption at the oil/water interface when hydrophobic tails orient towards the oil phase and hydrophilic head-groups align towards the water phase. Thus, *n*-decane and water molecules can penetrate into the hydrophobic and hydrophilic parts of a surfactant layer at the interface, leading to an increase in interfacial thicknesses.

Calculated values of h_{total} , h_{water} and h_{oil} for EHAC and CTAC at

different NaCl concentrations are shown in Fig. 10. Interestingly the observed patterns were different for both surfactants. Indeed, the total interfacial thickness (h_{total}) of water/EHAC/*n*-decane systems did not vary monotonically as a function of added salt, instead h_{total} clearly showed an inverse pattern to IFT (Fig. 10a). Indeed, h_{total} started to decrease when NaCl concentration exceeded 0.03 M (Fig. 10a). The same descending trend of Stern layer thickness was reported for fluid/solid adsorption as a function of NaCl concentration (up to 0.15 M) [63].

On the contrary, h_{total} of water/CTAC/*n*-decane systems decreased gradually in all brines (Fig. 10d). Moreover, h_{total} and h_{water} both decreased for all NaCl concentrations, while h_{oil} showed an increasing trend (Fig. 10e), due to incremental partitioning of CTAC molecules into the oil phase with increasing NaCl concentration.

Different results were reported in the literature regarding the dependence of IFT on h_{total} . For instance, it is generally accepted that an increase of interfacial thickness leads to an increase in the miscibility of two phases, with a consequent IFT reduction [43]. However, in the work of Qu et al. [64], it was shown that the thickness of water/surfactant/*n*-decane systems remained unchanged when temperature and salinity were increased, while IFT decreased. The authors explained this IFT descending trend by reducing the non-bonded potentials between water and surfactant molecules that led to a decrease of intermolecular forces [64]. Contrary to this, Jang et al. [24] reported a strong correlation between the interfacial thickness and the interfacial tension for *n*-decane/water interfaces in the presence of anionic surfactants. As such, the maximum broadening of the interfacial thickness in the presence of a surfactant was observed when IFT reached the minimum value. It was inferred that the low IFT was due to an increase of the phases' miscibility when surfactant was added.

To explain the trends obtained in our work, we further analyzed h_{water} and h_{oil} as a function of NaCl content (Fig. 10 b-f). As it can be seen in Fig. 10c, h_{water} of the water/EHAC/*n*-decane system broadened at low salt concentrations. This can be explained by taking into account that counter-ions penetrated into the headgroup layer adsorbed at the interface (Stern layer).

The co-adsorption of counter-ions, together with EHAC surfactant molecules at the interface, was supported by analyzing the average number of hydrogen bonds (n_{hb}) between surfactant head groups and water molecules (Fig. 11).

Generally, a hydrogen bond is an attractive electrostatic force acting between a hydrogen atom, bound covalently to a more electronegative atom, e.g. nitrogen, oxygen, fluorine. Hydrogen bonds are an important parameter to analyze as they play a critical role in controlling the solubilization of molecules containing oxygen and hydrogen in a water phase [20].

As can be seen from Fig. 11, the number of hydrogen bonds decreased rapidly with increasing salinity in EHAC systems. Thus, one can suggest that counter-ions bind with surrounding water molecules by ion-dipole interactions, leaving fewer water molecules to form bonds with the surfactant head groups. Therefore, the existence of counter-ions at the interface (when NaCl concentration was < 0.03 M) screens the electrostatic repulsion, and surfactant molecules are packed more tightly, reducing the IFT.

Interestingly, a further increase in NaCl concentration led to a decrease of n_{hb} , which indicates that fewer water molecules can form bonds with surfactant polar heads (Fig. 11). It is noteworthy that no hydrogen bonds were formed between CTAC and water molecules due to the fact that the nitrogen atom in the CTAC head group could not provide the lone pair of electrons for bond formation.

Notably, the same approach was used for predicting the adsorption of SDS and CTAB surfactant molecules in the presence of KCl [65] and NaCl [59].

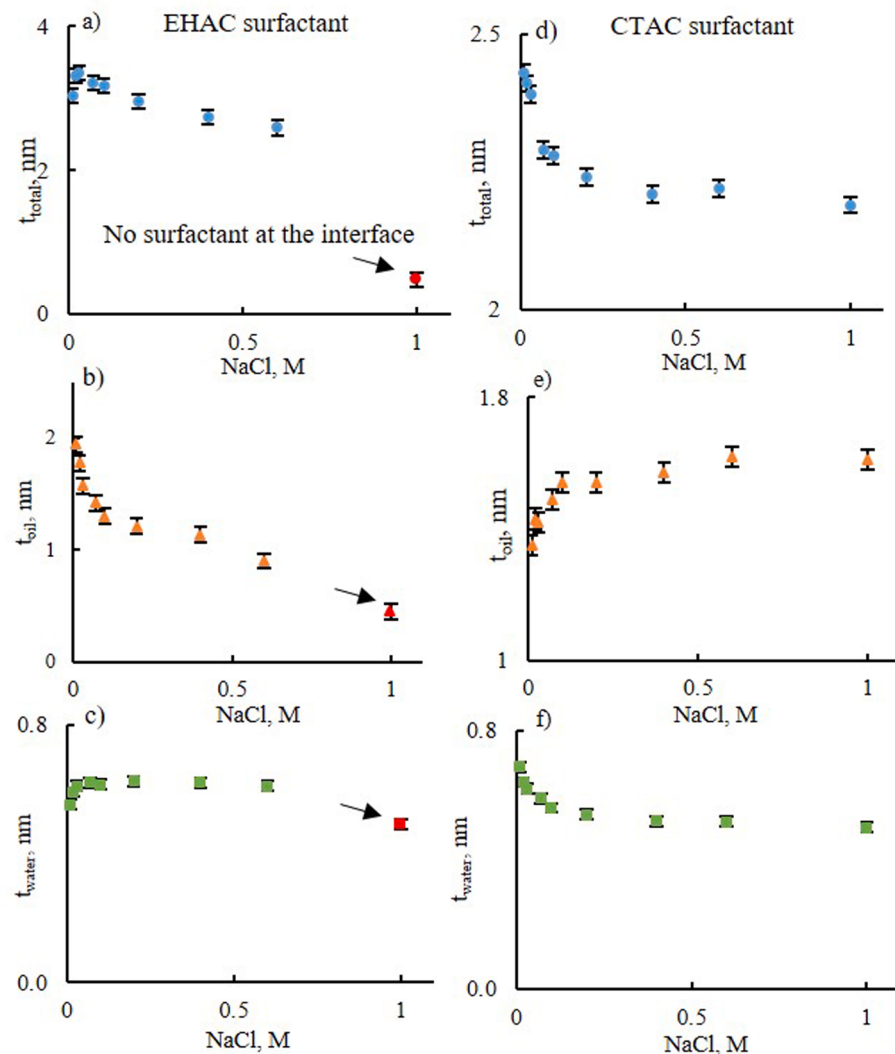


Fig. 10. Interfacial thickness as a function of NaCl concentration: total thickness (blue circles); oil thickness (orange triangles) and water thickness (green squares); (a)-(c) EHAC surfactant; (d)-(f) CTAC surfactant.

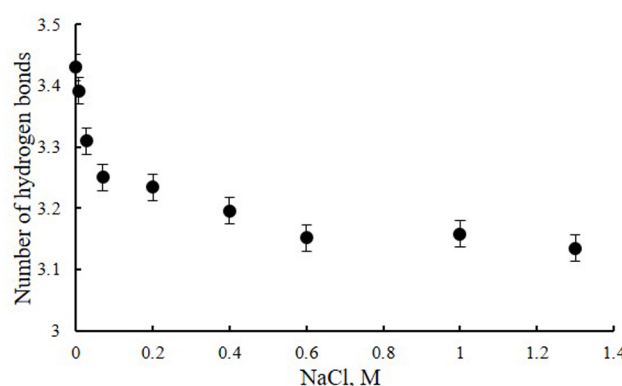


Fig. 11. An average number of hydrogen bonds (n_{hb}) between EHAC surfactant heads and water molecules as a function of NaCl concentration.

4. Conclusions

When selecting surfactants for enhanced oil recovery flooding, one should consider reservoir brine composition and temperature as two important factors that affect surfactant adsorption at the oil–water

interface, reduction of IFT, and consequently, improved oil production [32]. Screening surfactant properties at high salinity and temperature is thus essential to avoid failure of the whole recovery process. However, there is a lack of fundamental understanding of the detailed ion-surfactant-water-oil interactions at the atomistic level. This study thus investigated the influence of typical reservoir salinities and temperature on the adsorption process of two different cationic surfactants at the water/n-decane interface at the molecular level. We showed that surfactants had different IFT patterns as a salinity function due to their different headgroup architectures. So far, experimental studies [9,11,13] showed IFT passes through a minimum, illustrating two contrasting regions. From our work, we propose that the IFT trend of EHAC can be categorized into three regions, namely a first region where surfactant molecules adsorb at the interface, a second region where surfactant molecules desorb, and a third region where almost no surfactant molecules are left at the interface (and where thus micelle formation is facilitated). The increasing IFT trend (second region) was due to Na^+ ions positioned closer to the Stern layer. These Na^+ ions then contributed to the positive interfacial charge, resulting in the repulsion of surfactant molecules from the interface until no surfactant was left at the interface (third region).

However, the IFT of CTAC solutions increased for all salt concentrations examined. We attribute this to the decrease of CTAC solubility

in the aqueous phase caused by the salting-out effect. The slight migration of CTAC further into the oil phase was also verified by the interfacial thickness analysis. Moreover, temperature increase led to a decrease in IFT for all salt concentrations. However, IFT-salinity patterns resembled those measured at ambient temperature.

These results indicate that interactions between ions and surfactant molecules are competitive at the interface and cooperative in the bulk phase. The findings of this study thus provide important insights into the influence of ions in the interfacial zone, which can be used for screening surfactants that are favorable for enhanced oil recovery, ultimately leading to improved productivity.

CRediT authorship contribution statement

Anastasia A. Ivanova: Conceptualization, Methodology, Investigation, Software, Writing - original draft. **Alexey N. Cheremisin:** Writing - review & editing, Supervision. **Ahmed Barifcani:** Writing - review & editing, Resources, Supervision, Validation. **Stefan Iglauser:** Writing - review & editing, Resources, Supervision, Validation. **Chi Phan:** Writing - review & editing, Resources, Supervision, Validation.

Declaration of Competing Interest

The authors declare that they have no known competing financial interests or personal relationships that could have appeared to influence the work reported in this paper.

Acknowledgments

The authors gratefully acknowledge Curtin University and Skolkovo Institute of Science and Technology for providing a Ph.D. scholarship to support this research.

References

- [1] T. Cserháti, E. Forgács, G. Oros, Biological activity and environmental impact of anionic surfactants, Environ. Int. 28 (5) (2002) 337–348, [https://doi.org/10.1016/S0160-4120\(02\)00032-6](https://doi.org/10.1016/S0160-4120(02)00032-6).
- [2] R.N. Jordan, E.P. Nichols, A.B. Cunningham, The role of (bio)surfactant sorption in promoting the bioavailability of nutrients localized at the solid-water interface, Water Sci. Technol. 39 (1999) 91–98, [https://doi.org/10.1016/S0273-1223\(99\)00155-9](https://doi.org/10.1016/S0273-1223(99)00155-9).
- [3] C.A. Fauziah, A.Z. Al-Yaseri, R. Beloborodov, M.A.Q. Siddiqui, M. Lebedev, D. Parsons, H. Roshan, A. Barifcani, S. Iglauser, Carbon dioxide/brine, nitrogen/brine, and oil/brine wettability of montmorillonite, illite, and kaolinite at elevated pressure and temperature, Energy and Fuels 33 (1) (2019) 441–448, <https://doi.org/10.1021/acs.energyfuels.8b02845>.
- [4] E. Zdrali, G. Etienne, N. Smolentsev, E. Amstad, S. Roke, The interfacial structure of nano- and micron-sized oil and water droplets stabilized with SDS and Span80, J. Chem. Phys. 150 (2019), <https://doi.org/10.1063/1.5083844>.
- [5] S. Iglauser, Y. Wu, P. Shuler, Y. Tang, W.A. Goddard, New surfactant classes for enhanced oil recovery and their tertiary oil recovery potential, J. Petrol. Sci. Eng. 71 (1-2) (2010) 23–29, <https://doi.org/10.1016/j.petrol.2009.12.009>.
- [6] M.S. Kamal, I.A. Hussein, A.S. Sultan, Review on surfactant flooding: phase behavior, retention, IFT, and field applications, Energy Fuels 31 (2017) 7701–7720, <https://doi.org/10.1021/acs.energyfuels.7b00353>.
- [7] L.C. Price, Aqueous solubility of petroleum as applied to its origin and primary migration, AAPG Bull. 60 (1976) 213–244, <https://doi.org/10.1306/83D922A8-16C7-11D7-8645000102C1865D>.
- [8] A.Z. Hezave, S. Dorostkar, S. Ayatollahi, M. Nabipour, B. Hemmateenejad, Dynamic interfacial tension behavior between heavy crude oil and ionic liquid solution (1-dodecyl-3-methylimidazolium chloride ([C12mim] [Cl] + distilled or saline water/heavy crude oil)) as a new surfactant, J. Mol. Liq. 187 (2013) 83–89, <https://doi.org/10.1016/j.molliq.2013.05.007>.
- [9] S. Kumar, A. Mandal, Studies on interfacial behavior and wettability change phenomena by ionic and non-ionic surfactants in presence of alkalis and salt for enhanced oil recovery, Appl. Surf. Sci. 372 (2016) 42–51, <https://doi.org/10.1016/j.apsusc.2016.03.024>.
- [10] L.S.C. Wan, P.K.C. Poon, Effect of salts on the surface/interfacial tension and critical micelle concentration of surfactants, J. Pharm. Sci. 58 (12) (1969) 1562–1567, <https://doi.org/10.1002/jps.2600581238>.
- [11] Z. Liu, L. Zhang, X. Cao, X. Song, Z. Jin, L. Zhang, S. Zhao, Effect of electrolytes on interfacial tensions of alkyl ether carboxylate solutions, Energy Fuels 27 (2013) 3122–3129, <https://doi.org/10.1021/ef400458q>.
- [12] J.-M. Bai, W.-Y. Fan, G.-Z. Nan, S.-P. Li, B.-S. Yu, Influence of interaction between heavy oil components and petroleum sulfonate on the oil–water interfacial tension, J. Disper. Sci. Technol. 31 (4) (2010) 551–556, <https://doi.org/10.1080/01932690903167475>.
- [13] A. Bera, A. Mandal, B.B. Guha, Synergistic effect of surfactant and salt mixture on interfacial tension reduction between crude oil and water in enhanced oil recovery, J. Chem. Eng. Data 59 (2014) 89–96, <https://doi.org/10.1021/je400850c>.
- [14] Z. Zhao, C. Bi, Z. Li, W. Qiao, L. Cheng, Interfacial tension between crude oil and decylmethylnaphthalene sulfonate surfactant alkali-free flooding systems, Colloids Surfaces A Physicochem. Eng. Asp. 276 (1-3) (2006) 186–191, <https://doi.org/10.1016/j.colsurfa.2005.10.036>.
- [15] G. Liu, R. Li, Y. Wei, F. Gao, H. Wang, S. Yuan, C. Liu, Molecular dynamics simulations on tetraalkylammonium interactions with dodecyl sulfate micelles at the air/water interface, J. Mol. Liq. 222 (2016) 1085–1090, <https://doi.org/10.1016/j.molliq.2016.08.009>.
- [16] G. Gao, C.V. Nguyen, C.M. Phan, Molecular arrangement between electrolyte and alcohol at the air/water interface, J. Mol. Liq. 242 (2017) 859–867, <https://doi.org/10.1016/j.molliq.2017.07.083>.
- [17] H. Kuhn, H. Rehage, Molecular orientation of monododecyl pentaethylene glycol at water/air and water/oil interfaces. A molecular dynamics computer simulation study, Colloid Polym. Sci. 278 (2000) 114–118, [10.1007/s003960050019](https://doi.org/10.1007/s003960050019).
- [18] T. Zhao, G. Xu, S. Yuan, Y. Chen, H. Yan, Molecular dynamics study of alkyl benzene sulfonate at air/water interface: effect of inorganic salts, J. Phys. Chem. B 114 (2010) 5025–5033, <https://doi.org/10.1021/jp907438x>.
- [19] H. Domínguez, Computer simulations of surfactant mixtures at the liquid/liquid interface, J. Phys. Chem. B 106 (23) (2002) 5915–5924, <https://doi.org/10.1021/jp011403c>.
- [20] A.A. Ivanova, A.N. Cheremisin, A. Barifcani, S. Iglauser, C. Phan, Molecular insights in the temperature effect on adsorption of cationic surfactants at liquid/liquid interfaces, J. Mol. Liq. 299 (2020) 1–9, <https://doi.org/10.1016/j.molliq.2019.112104>.
- [21] Y. Li, X.J. He, X.L. Cao, Y.H. Shao, Z.Q. Li, F.L. Dong, Mesoscopic simulation study on the efficiency of surfactants adsorbed at the liquid/liquid interface, Mol. Simul. 31 (14-15) (2005) 1027–1033, <https://doi.org/10.1080/08927020500411948>.
- [22] K.J. Schweighofer, U. Essmann, M. Berkowitz, Structure and dynamics of water in the presence of charged surfactant monolayers at the water–ccl4 interface. A molecular dynamics study, J. Phys. Chem. B 101 (50) (1997) 10775–10780, <https://doi.org/10.1021/jp971865a>.
- [23] C.D. Bruce, M.L. Berkowitz, L. Perera, D.E. Forbes, Molecular dynamics simulation of sodium dodecyl sulfate micelle in water: micellar structural characteristics and counterion distribution, J. Phys. Chem. B 106 (2002) 3788–3793, <https://doi.org/10.1021/jp013616z>.
- [24] S.S. Jang, S.T. Lin, P.K. Maiti, M. Blanco, W.A. Goddard III, Molecular dynamics study of a surfactant-mediated decane-water interface: effect of molecular architecture of alkyl benzene sulfonate, J. Phys. Chem. B 108 (2004) 12130–12140, <https://doi.org/10.1021/jp048773n>.
- [25] M.H. Badizad, M.M. Koleini, R. Hartkamp, S. Ayatollahi, M.H. Ghazanfari, How do ions contribute to brine-hydrophobic hydrocarbon Interfaces? An in silico study, J. Colloid Interface Sci. 575 (2020) 337–346, <https://doi.org/10.1016/j.jcis.2020.04.060>.
- [26] F. Goodarzi, S. Zendehboudi, Effects of salt and surfactant on interfacial characteristics of water/oil systems: molecular dynamic simulations and dissipative particle dynamics, Ind. Eng. Chem. Res. 58 (2019) 8817–8834, <https://doi.org/10.1021/acs.iecr.9b00504>.
- [27] J.B. Maillet, V. Lachet, P.V. Coveneay, Large scale molecular dynamics simulation of self-assembly processes in short and long chain cationic surfactants, Phys. Chem. Chem. Phys. 23 (1999) 5277–5290, <https://doi.org/10.1039/A905216j>.
- [28] A.A. Ivanova, C. Phan, A. Barifcani, S. Iglauser, A.N. Cheremisin, Effect of nanoparticles on viscosity and interfacial tension of aqueous surfactant solutions at high salinity and high temperature, J. Surfactants Deterg. (2019), <https://doi.org/10.1002/jscd.12371>.
- [29] A.A. Ivanova, A.N. Cheremisin, M.Y. Spasennykh, Application of nanoparticles in chemical EOR, EAGE Conf. Proc. (2017), <https://doi.org/10.3997/2214-4609.201700247>.
- [30] A.R. van Buuren, S.J. Marrink, H.J.C. Berendsen, A molecular dynamics study of the decane/water interface, J. Phys. Chem. 97 (36) (1993) 9206–9212.
- [31] J.L. Rivera, C. McCabe, P.T. Cummings, Molecular simulations of liquid-liquid interfacial properties: water-n-alkane and water-methanol-n-alkane systems, Phys. Rev. E 67 (2002), <https://doi.org/10.1103/PhysRevE.67.011603>.
- [32] D.W. Green, G.P. Willhite, Enhanced Oil Recovery, SPE Textbook Series. (1998).
- [33] H.Y. Cai, Y. Zhang, Z.Y. Liu, J.G. Li, Q.T. Gong, Q. Liao, L. Zhang, S. Zhao, Molecular dynamics simulation of binary betaine and anionic surfactant mixtures at decane - Water interface, J. Mol. Liq. 266 (2019) 82–89, <https://doi.org/10.1016/j.molliq.2018.06.047>.
- [34] C.M. Phan, C.V. Nguyen, S.-I. Yusa, N.L. Yamada, Synergistic adsorption of MIBC/CTAB mixture at the air/water interface and applicability of Gibbs adsorption equation, Langmuir 30 (20) (2014) 5790–5796, <https://doi.org/10.1021/la500721d>.
- [35] C.M. Phan, T.N. Le, C.V. Nguyen, S.-I. Yusa, Modeling adsorption of cationic surfactants at air/water interface without using the Gibbs equation, Langmuir 29 (15) (2013) 4743–4749, <https://doi.org/10.1021/la3046302>.
- [36] P.D.T. Huibers, Quantum-chemical calculations of the charge distribution in ionic surfactants, Langmuir 15 (22) (1999) 7546–7550, <https://doi.org/10.1021/la9903671>.
- [37] W.R.P. Scott, P.H. Hünenberger, I.G. Tironi, A.E. Mark, S.R. Billeter, J. Fennen, A. E. Torda, T. Huber, P. Krüger, W.F. van Gunsteren, The GROMOS biomolecular

- simulation program package, *J. Phys. Chem. A* 103 (19) (1999) 3596–3607, <https://doi.org/10.1021/jp984217f>.
- [38] J. Hermans, H.J.C. Berendsen, W.F. Van Gunsteren, J.P.M. Postma, A consistent empirical potential for water–protein interactions, *Biopolymers* 23 (8) (1984) 1513–1518, <https://doi.org/10.1002/bip.360230807>.
- [39] H.J.C. Berendsen, J.R. Grigera, T.P. Straatsma, The missing term in effective pair potentials, *J. Phys. Chem.* 91 (24) (1987) 6269–6271.
- [40] G. Hantal, M. Suga, G. Horvai, P. Jedlovszky, Contribution of different molecules and moieties to the surface tension in aqueous surfactant solutions, *J. Phys. Chem. C* 123 (27) (2019) 16660–16670, <https://doi.org/10.1021/acs.jpcc.9b02553>.
- [41] Y. Li, X. He, X. Cao, G. Zhao, X. Tian, X. Cui, Molecular behavior and synergistic effects between sodium dodecylbenzene sulfonate and Triton X-100 at oil/water interface, *J. Colloid Interface Sci.* 307 (1) (2007) 215–220, <https://doi.org/10.1016/j.jcis.2006.11.026>.
- [42] B. Hess, C. Kutzner, D. van der Spoel, E. Lindahl, GROMACS 4: Algorithms for highly efficient, load-balanced, and scalable molecular simulation, *J. Chem. Theory Comput.* 4 (2008) 435–447, <https://doi.org/10.1021/ct700301q>.
- [43] M.J. Rosen, *Surfactants and interfacial phenomena*, 3rd ed., John Wiley & Sons Inc., Hoboken, NJ, 2004.
- [44] W.K. Kegel, H.N.W. Lekkerkerker, Phase behaviour of an ionic microemulsion system as a function of the cosurfactant chain length, *Colloids Surfaces A Physicochem. Eng. Asp.* 76 (1993) 241–248, [https://doi.org/10.1016/0927-7757\(93\)80084-R](https://doi.org/10.1016/0927-7757(93)80084-R).
- [45] N. Anton, P. Saulnier, A. Béduneau, J.-P. Benoit, Salting-out effect induced by temperature cycling on a water/non-ionic surfactant/oil system, *J. Phys. Chem. B* 111 (14) (2007) 3651–3657, <https://doi.org/10.1021/jp0664768>.
- [46] B.P. Binks, A. Espert, P.D.I. Fletcher, L. Soubiran, Phase behaviour of microemulsions stabilised by double chain cationic surfactants and alcohol co-surfactants, *Colloids Surfaces A Physicochem. Eng. Asp.* 212 (2–3) (2003) 135–145, [https://doi.org/10.1016/S0927-7757\(02\)00300-X](https://doi.org/10.1016/S0927-7757(02)00300-X).
- [47] J. Zhang, L.u. Li, J. Wang, H. Sun, J. Xu, D. Sun, Double inversion of emulsions induced by salt concentration, *Langmuir* 28 (17) (2012) 6769–6775, <https://doi.org/10.1021/la300695v>.
- [48] R. Aveyard, S.M. Saleem, Interfacial tensions at alkane-aqueous electrolyte interfaces, *J. Chem. Soc., Faraday Trans. 1* (72) (1976) 1609–1617, <https://doi.org/10.1039/F19767201609>.
- [49] H.I. Okur, Y. Chen, D.M. Wilkins, S. Roke, The Jones-Ray effect reinterpreted: Surface tension minima of low ionic strength electrolyte solutions are caused by electric field induced water/water correlations, *Chem. Phys. Lett.* 684 (2017) 433–442, <https://doi.org/10.1016/j.cplett.2017.06.018>.
- [50] C.M. Phan, C.V. Nguyen, T.T.T. Pham, Molecular arrangement and surface tension of alcohol solutions, *J. Phys. Chem. B* 120 (2016) 3914–3919, <https://doi.org/10.1021/acs.jpcb.6b01209>.
- [51] C.V. Nguyen, C.M. Phan, H.M. Ang, H. Nakahara, O. Shibata, Y. Moroi, Molecular dynamics investigation on adsorption layer of alcohols at the air/brine interface, *Langmuir* 31 (2015) 50–56, <https://doi.org/10.1021/la504471>.
- [52] P.K. Yuet, D. Blankschtein, Molecular dynamics simulation study of water surfaces: comparison of flexible water models, *J. Phys. Chem. B* 114 (2010) 13786–13795, <https://doi.org/10.1021/jp1067022>.
- [53] M. Puerto, G.J. Hirasaki, C.A. Miller, J.R. Barnes, Surfactant systems for EOR in high-temperature, high-salinity environments, *SPE J.* 17 (2010) 11–19, <https://doi.org/10.2118/129675-PA>.
- [54] W.M. Haynes (Ed.), *CRC Handbook of Chemistry and Physics*, CRC Press, Florida, 2014.
- [55] I. Benjamin, Molecular structure and dynamics at liquid-liquid interfaces, *Annu. Rev. Phys. Chem.* 48 (1) (1997) 407–451, <https://doi.org/10.1146/annurev.physchem.48.1.407>.
- [56] N. Ikeda, M. Aratono, K. Motomura, Thermodynamic study on the adsorption of sodium chloride at the water/hexane interface, *J. Colloid Interface Sci.* 149 (1) (1992) 208–215, [https://doi.org/10.1016/0021-9797\(92\)90405-B](https://doi.org/10.1016/0021-9797(92)90405-B).
- [57] M.S. Alam, A.M. Siddiqi, V. Mythili, M. Priyadarshini, N. Kamely, A.B. Mandal, Effect of organic additives and temperature on the micellization of cationic surfactant cetyltrimethylammonium chloride: evaluation of thermodynamics, *J. Mol. Liq.* 199 (2014) 511–517, <https://doi.org/10.1016/j.molliq.2014.09.026>.
- [58] W. Humphrey, A. Dalke, K. Schulten, VMD: Visual molecular dynamics, *J. Mol. Graphics* 14 (1996) 33–38, [https://doi.org/10.1016/0263-7855\(96\)00018-5](https://doi.org/10.1016/0263-7855(96)00018-5).
- [59] P. Warszyński, K. Lunkenheimer, G. Czichocki, Effect of counterions on the adsorption of ionic surfactants at fluid-fluid interfaces, *Langmuir* 18 (7) (2002) 2506–2514, <https://doi.org/10.1021/la010381->.
- [60] S. Zeppieri, J. Rodríguez, A.L. López de Ramos, Interfacial tension of alkane + water systems, *J. Chem. Eng. Data* 46 (5) (2001) 1086–1088, <https://doi.org/10.1021/je000245r>.
- [61] N.G. Tsierkezos, I.E. Molinou, Thermodynamic properties of water + ethylene glycol at 283.15, 293.15, 303.15, and 313.15 K, *J. Chem. Eng. Data* 43 (6) (1998) 989–993, <https://doi.org/10.1021/je9800914>.
- [62] D.M. Mitrinović, A.M. Tikhonov, M. Li, Z. Huang, M.L. Schlossman, Noncapillary-wave structure at the water-alkane interface, *Phys. Rev. Lett.* 85 (3) (2000) 582–585, <https://doi.org/10.1103/PhysRevLett.85.582>.
- [63] M.A. Brown, A. Goel, Z. Abbas, Effect of electrolyte concentration on the Stern layer thickness at a charged interface, *Angew. Chem. Int. Ed.* 55 (11) (2016) 3790–3794, <https://doi.org/10.1002/anie.201512025>.
- [64] G. Qu, C. Xue, M. Zhang, S. Liang, Y. Han, W. Ding, Molecular dynamics simulation of sulfobetaine-type zwitterionic surfactants at the decane/water interface: structure, interfacial properties, *J. Disper. Sci. Technol.* 37 (12) (2016) 1710–1717, <https://doi.org/10.1080/01932691.2015.1135400>.
- [65] Z. Adamczyk, G. Para, P. Warszyński, Influence of ionic strength on surface tension of cetyltrimethylammonium bromide, *Langmuir* 15 (24) (1999) 8383–8387, <https://doi.org/10.1021/la990241o>.